SiRNA-loaded multi-shell nanoparticles incorporated into a multilayered film as a reservoir for gene silencing

Xin Zhang [a,b,1], Anna Kovtun [c,1], Carlos Mendoza-Palomares [a,b,1], Mustapha Oulad-Abdelghani [d,1], Florence Fioretti [a,b], Simon Rinckenbach [a,b], Didier Mainard [e], Matthias Epple [c,*], Nadia Benkirane-Jessel [a,b,e,*]

[a] Institut National de la Santé et de la Recherche Médicale, INSERM, Unité 977, Faculté de Médecine, 11 Rue Humann, 67085 Strasbourg Cedex, France
[b] Faculté de Chirurgie, Dentaire de l'Université Louis Pasteur (UdS), Strasbourg Cedex 67000, France
[c] Institute of Inorganic Chemistry and Center for Nanointegration Duisburg-Essen (CeNIDE), University of Duisburg-Essen, Universitaetsstrasse 5-7, D-45117 Essen, Germany
[d] Institut de Génétique et de Biologie Moléculaire et Cellulaire (IGBMC), Institut Clinique de la Souris (ICS), Centre National de la Recherche Scientifique
(CNRS)/INSERM/UdS, Collège de France, BP 10142, Strasbourg Cedex 67404, France
[e] Hôpital Central, «CHIRURGIE ORTHOPEDIQUE ET TRAUMATOLOGIE», 29 Avenue du Maréchal de Lattre de Tassigny, and CNRS, UMR 7561, Nancy 54000, France

ARTICLE INFO

ABSTRACT

In this study, we presented a new type of coating based on polyelectrolyte multilayers containing sequentially adsorbed active shRNA calcium phosphate nanoparticles for locally defined and temporarily variable gene silencing. Therefore, we investigated multi-shell calcium phosphate-shRNA nanoparticles embedded into a polyelectrolyte multilayer for gene silencing. As model system, we synthesized triple-shell calcium phosphate-shRNA nanoparticles (NP) and prepared polyelectrolyte multilayers films made of nanoparticles and poly-(L-lysine) (PLL). The biological activities of these polyelectrolyte multilayers films were tested by the production of osteopontin and osteocalcin in the human osteoblasts (HOb) which were cultivated on the PEM films. This new strategy can be used to efficiently control the bone formation and could be applicable in tissue engineering.

© 2010 Elsevier Ltd. All rights reserved.

1. Introduction

RNA interference (RNAi) is a very promising approach for the treatment of inherited and acquired diseases [1–4] because it can selectively inhibit the biosynthesis of proteins in cells. RNAi can be induced by the introduction of synthetic siRNA or by intracellular generation of siRNA from vector-driven expression of the precursor small hairpin RNA (shRNA) [5]. The shRNA effects are longer-lived compared with siRNA because the latter is continually produced within the cells.

The major challenge for this approach is to find an efficient delivery method for shRNA into cells [2]. Effective viral systems were developed to achieve this goal, but there are several concerns about the use of viruses, mainly the toxicity of viruses and the potential for generating a strong immune response due to the proteinaceous capsid [5–7]. Therefore, a suitable non-viral vector must be employed. Different systems were developed, *e.g.* polymers [8,9], liposomes [10,11], peptides [12,13], or inorganic nanoparticles like silica, magnetite, clay, gold, and calcium phosphate [14]. Such systems serve as a vector for active molecules which can pass through the cell membrane, escape from cytoplasmatic vesicles, and then reach their target in the cytoplasm.

We have recently shown that custom-made DNA-functionalized calcium phosphate nanoparticles can be used for cell transfection [15]. Their transfection efficiency can be increased if DNA is incorporated into the calcium phosphate particle where it is prevented from intracellular degradation by nucleases [16,17]. Calcium phosphate is advantageous compared to other types of nanoparticles due to its easy preparation [18], its high biocompatibility, and its good biodegradability in biological systems [19]. Note that cationic polymers and liposomes are often toxic towards cells [14].

The layer-by-layer (LbL) buildup of polyelectrolyte membrane films (PEM films) consisting of oppositely charged polyelectrolytes [20] offers new opportunities for the preparation of functionalized biomaterial coatings. This technique allows the preparation of

* Corresponding authors. Institut National de la Santé et de la Recherche Médicale, INSERM, Unité 977, Faculté de Médecine, 11 Rue Humann, 67085 Strasbourg Cedex, France. Fax: +33 3 90243379.
E-mail addresses: matthias.epple@uni-due.de (M. Epple), nadia.jessel@medecine.u-strasbg.fr (N. Benkirane-Jessel).
[1] All authors contributed equally to this work.
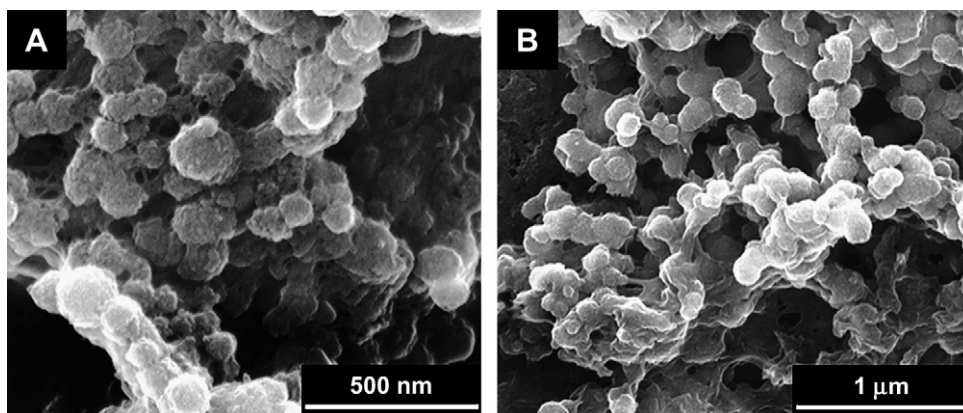
Fig. 1. SEM images of triple-shell calcium phosphate-shRNA nanoparticles functionalized with shRNA against osteopontin (Spp1) (A) and shRNA against osteocalcin (Bglap-rs1) (B).

supramolecular nano-architectures [21–26] with the specific ability to control cell activation [21,24–26], and may also play a role in the development of local drug delivery systems [22]. Peptides and proteins, either chemically bound, physically adsorbed or embedded into PEM films, retain their biological activities [27–29].

In the last years, it has also been shown that PEM films are efficient to deliver plasmid DNA (pDNA). Lynn et al. found that multilayered films consisting of naked pDNA and a degradable polyamine were able to efficiently release pDNA from the surfaces under physiological conditions which led to a subsequent in vitro transfection of adherent cells [30]. Recently, we have also shown that multilayered films can act as a reservoir of pre-complexed DNA [31], and demonstrated clearly the multiple and time-scheduled in situ DNA delivery mediated by β-cyclodextrin embedded into a PEM film [19].

Until now, no study was directed to multilayers containing siRNA or shRNA nanoparticles which possess gene silencing activity. The aim of this work is to present a new type of coating based on polyelectrolyte multilayers containing sequentially adsorbed active shRNA calcium phosphate nanoparticles for locally defined and temporarily variable gene silencing. Therefore, we investigated multi-shell calcium phosphate-shRNA nanoparticles embedded into a polyelectrolyte multilayer for gene silencing. As model system, we synthesized triple-shell calcium phosphate-shRNA nanoparticles (NP) and prepared PEM films made of nanoparticles and poly-(L-lysine) (PLL).

shRNAs against osteopontin ("Spp1") or osteocalcin ("Bglap-rs1") were employed. Triple-shell calcium phosphate-Spp1-nanoparticles and triple-shell calcium phosphate-Bglap-rs1-nanoparticles were synthesized to inhibit the osteopontin and osteocalcin expression, respectively. Osteopontin is an extracellular structural bone protein, and osteocalcin is a noncollagenous bone protein. They are typically employed as biomarkers for bone formation process. The biological activities of these PEM films were tested by the production of osteopontin and osteocalcin in the human osteoblasts (HOb) which were cultivated on the PEM films.

2. Materials and methods

2.1. Materials

Poly-L-lysine hydrobromide (PLL, $M_W = 30$ kDa) and YOYO-1 (1,1'-(4,4,8,8-tetramethyl-4,8-diazaundecamethylene)bis[4-{(3-methylbenz-1,3-oxazol-2-yl)methylidine}-1,4-dihydroquinolinium]) tetraiodide were purchased from Sigma (St. Quentin Fallavier, France). Bisbenzimide H 33258 (Hoechst) used for microscopy was purchased from Invitrogen, Molecular Probes. ShRNA (mouse Spp1 and Bglap-rs1) was purchased from SuperArray Inc.

2.2. Preparation of multi-shell calcium phosphate-shRNA nanoparticles

Multi-shell (triple-shell) calcium phosphate-shRNA nanoparticles were prepared by a precipitation method under constant stirring as described earlier [17]. We used two types of shRNA: Spp1 for the silencing of osteopontin expression and Bglap-rs1 for silencing of osteocalcin expression.

First, aqueous solutions of $Ca(NO_3)_2 \cdot 4H_2O$ (6.25 mM) and $(NH_4)_2HPO_4$ (3.74 mM) were adjusted to pH 9 with 0.1 M NaOH and then rapidly mixed with a peristaltic pumps into a plastic vessel. Immediately thereafter, 1 mL of the mixture was taken with an Eppendorf pipette and mixed with 0.1 mg of shRNA dissolved in water (the concentrations were 0.75 mg mL^{-1} and 0.83 mg mL^{-1} for Spp1 and Bglap-rs1, respectively). These nanoparticles consisted of a calcium phosphate core and an outer layer of shRNA for electrostatic and steric functionalization and are denoted "single-shell" in the following.

To obtain multi-shell particles, the 0.5 mL of $Ca(NO_3)_2 \cdot 4H_2O$ solution (6.25 mM) and 0.5 mL of $(NH_4)_2HPO_4$ solution (3.74 mM) were added to the dispersed single-shell nanoparticles. Immediately thereafter, we added 0.1 mg of shRNA dissolved in water as outer layer of the particles (the concentrations were 0.75 mg mL^{-1} and 0.83 mg mL^{-1} for Spp1 and Bglap-rs1, respectively). These "triple-shell" particles consisted of a calcium phosphate core and further layers of shRNA, calcium phosphate and shRNA.

2.3. Scanning electron microscopy

Scanning electron microscopy (SEM) was carried out with ESEM Quanta 400 FEG instrument with gold–palladium-sputtered samples. 15 μL of the nanoparticle dispersion was dried on the aluminum holder for 30 min at 37 °C and then sputtered with an EMITECH Sputter Coater K550 (Ashford, UK) for 30 s with gold–palladium.

2.4. Dynamic light scattering

The average size of the nanoparticles was determined with a Zetasizer Nano ZS (Malvern Instruments, Malvern, UK) with the following specifications: medium
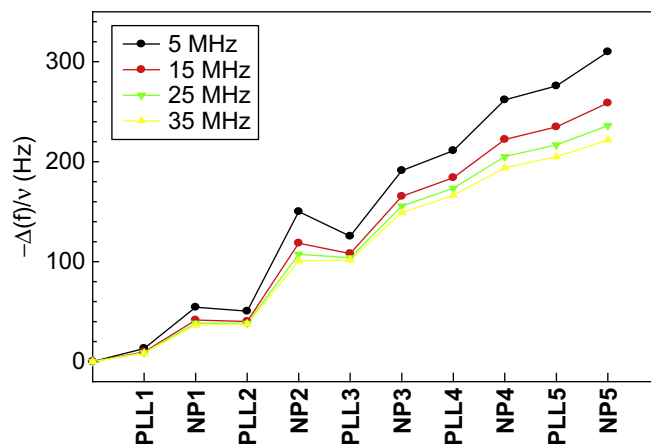
Fig. 2. Quartz crystal microbalance measurement. Frequency shifts ($-\Delta f/v$ at 5, 15, 25 and 35 MHz) are shown as a function of sequential layer deposition of PLL and calcium phosphate nanoparticles (NP).
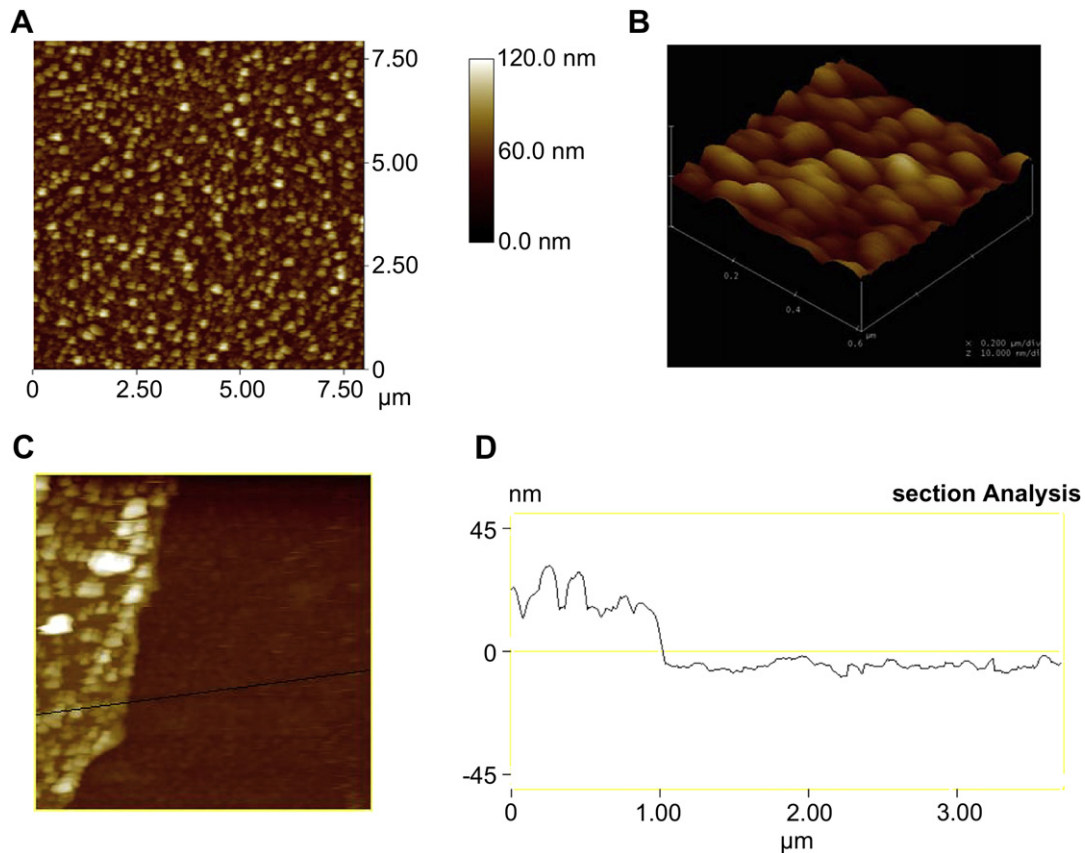
Fig. 3. *In situ* AFM images of (PLL–NP)$_6$ LBL polyelectrolyte films deposited on a quartz surface. A and B: Height mode AFM images; C: observation of a scratch performed on the surface (the scratched zone is located on the right part of the image); D: profile section of the scratched film along the black line drawn on image C.

viscosity 0.8872 cP, refractive index (RI) medium 1.33, RI particle 1.14, scattering angle 90°, temperature 25 °C. The zeta potential of the complexes was measured with the following specifications: medium viscosity 0.8872 cP, dielectric constant 78.5, scattering angle 90°, temperature 25 °C.

2.5. Polyelectrolyte multilayered film preparation

Polyelectrolyte multilayered films were prepared on glass coverslips (CML, France) pre-treated with 10^{-2} M SDS and 0.12 M HCl for 15 min at 100 °C, and then extensively rinsed with deionized water. Then glass slides were placed into a 24-well plate. Next, a film consisting of alternating layers of poly(L-lysine) (PLL) and nanoparticles (NP) (PLL–NP)$_n$ was built up by alternated immersions for 10 min in the corresponding solutions (300 μL each time). The PLL solution contained 0.5 mg mL^{-1} PLL in 0.15 M NaCl at pH 7.4, and the nanoparticle dispersion consisted of 8 μg nanoparticles in deionized water. After each layer deposition, the coverslips were rinsed three times during 5 min with deionized water. PLL was deposited as the last layer, so that cells could adhere to it. After the deposition of n bilayers, the films were dried and sterilised under UV light for 15 min. Before cell seeding, the films were put in contact with 1 mL of cell culture medium without serum for 24 h.

2.6. Quartz crystal microbalance

The films were monitored *in situ* with a quartz crystal microbalance using an axial flow chamber QAFC 302 (QCM-D, D300, Q-Sense, Götenborg, Sweden). QCM works by measuring the resonance frequency shift (Δf) of a quartz crystal induced by polyelectrolyte or protein adsorption onto the crystal in comparison to the crystal in contact with buffer. Changes in the resonance frequencies were measured at the third overtone ($v = 3$), corresponding to the 15 MHz resonance frequency. A shift in $\Delta f/v$ can be related in a first approximation to a variation of the mass adsorbed to the crystal by the Sauerbrey relation: $m = -C\,\Delta f/v$, where C is a constant characteristic of the crystal used (in our case: $C = 17.7$ ng cm^{-2} Hz^{-1}). The details of the methodology applied in the present work were described elsewhere [32].

2.7. Atomic force microscopy

The film deposited by QCM is imaged in liquid condition in deflection mode using a Nanoscope IV from Veeco (Santa Barbara, CA, USA). Cantilevers with a spring constant of 0.01 N m^{-1} and with silicon nitride tips were used (Model MSCT-AUHW Veeco). Deflection mode images are scanned at a scan rate of 2 Hz with a resolution of 512 × 512 pixels.

2.8. Cell culture

Human Osteoblasts (HOb) were grown in Osteoblast Growth Medium (Cell Applications, Inc.). Cells were maintained at 37 °C in 5% CO$_2$ humidified atmosphere.

2.9. Immunofluorescence

After the cultivation on the layers for 21 days, the HOb cells were fixed with 2% paraformaldehyde in phosphate buffered saline (PBS) for 4 min at room temperature and incubated twice for 10 min with PBS containing 0.1% Triton X-100 (PBS-Tx) [33]. After a PBS wash, the cells were incubated overnight at room temperature with goat anti-osteopontin or osteocalcin antibodies, respectively, as primary antibody diluted to 5 μg mL^{-1} in PBS. After overnight incubation at room temperature, the cells were washed with PBS-Tx and incubated with a donkey anti-goat secondary antibody diluted at 1/500 in PBS-Tx for 1 h at room temperature. The cells were washed with
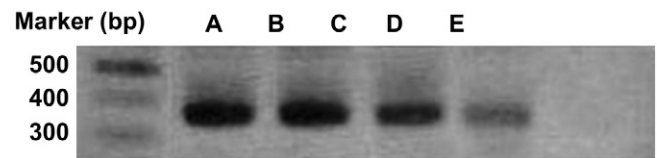
Fig. 4. RT-PCR analysis of osteocalcin expression in osteoblasts cultured for 21 days. A: without shRNA; B: in contact with the multilayered film without shRNA; C: with shRNA-functionalized nanoparticles in dispersion; D: with shRNA-functionalized nanoparticles incorporated into the multilayered film (PLL-shRNA NP)$_6$; E: RT-PCR without any RNA as control. The total RNA was isolated and analyzed by RT-PCR. The position of DNA length markers is indicated and the osteocalcin-amplified band is detected at 370 bp. Control experiments (not shown) on the same RNA samples did not show any significant variation in the content of the invariant 36B4 RNA.
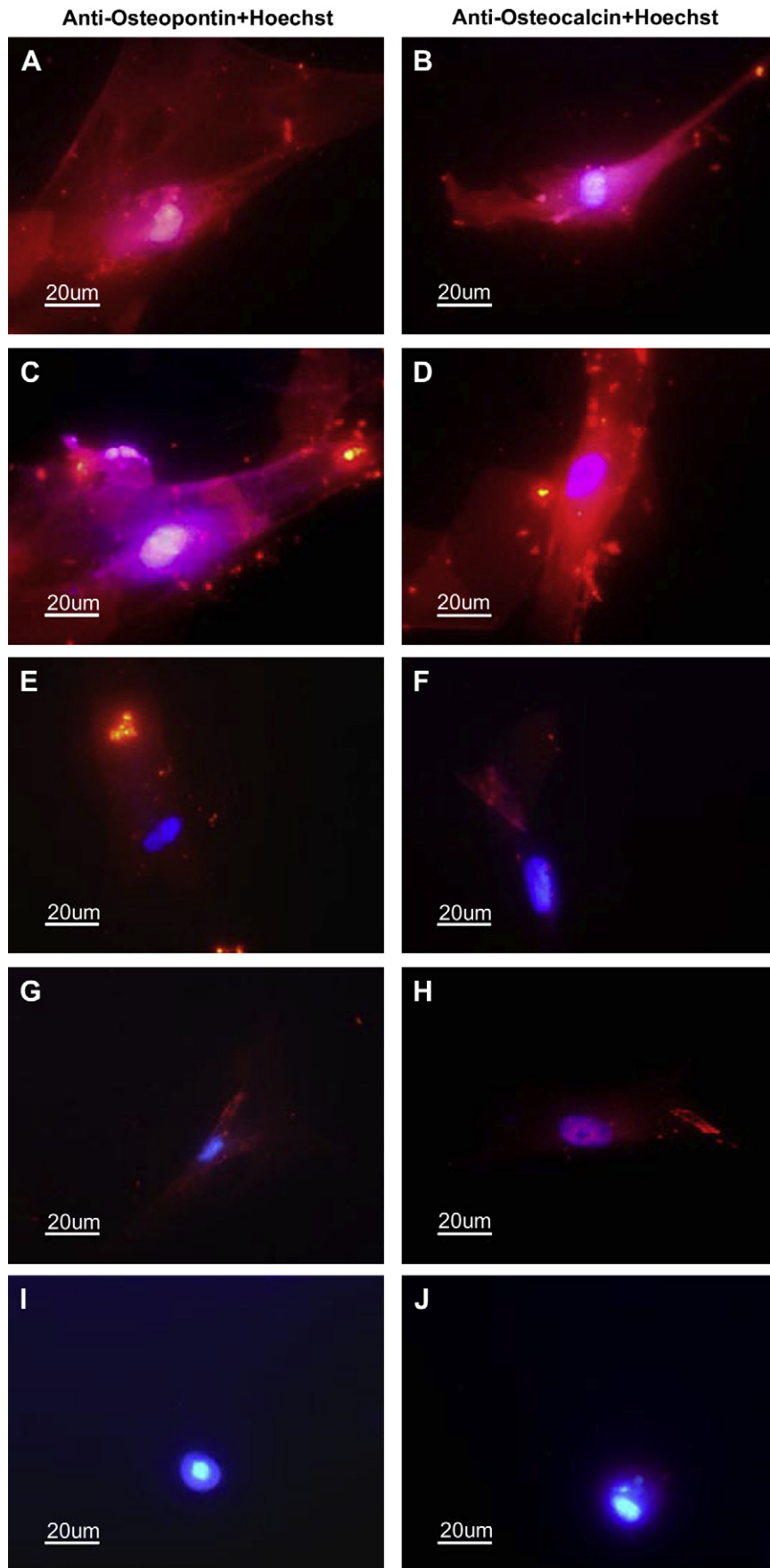
Fig. 5. Osteopontin and osteocalcin expression in osteoblasts cultured for 21 days in untreated cells (A and B), in dispersion in the presence of free dissolved shRNA (C and D), in the presence of dispersed shRNA-functionalized nanoparticles (E and F), on (PLL-shRNA NP)$_1$ films (G and H), and on (PLL-shRNA NP)$_6$ (I and J) films. The expression of osteopontin and Osteocalcin was detected by using goat antibody as primary antibody and Cy3-conjugated donkey anti-goat as secondary antibody. Nuclei were visualized by Hoechst 33258 staining (Blue).

PBS-Tx, rinsed with PBS, and counterstained with Hoechst 33258 DNA dye (5 μg mL^{-1} bisbenzimide; Sigma) for 20 s.

The cells were covered with mounting medium (Vector Laboratories Inc. Burlingame, CA) and analyzed by fluorescence microscopy. Immunostaining for osteopontin and osteocalcin expressing cells (red) was monitored with a cool snap camera coupled to a Leica DRB microscope using a specific CY3 filter. We counted the cells by labelling the cell nucleus with Hoechst 33258 DNA dye both for dispersion and multilayers. The cell numbers were approximately the same. The amounts of shRNA NP used in dispersion and multilayer were the same.

2.10. Reverse-transcriptase polymerase chain reaction

Total RNA was extracted from osteoblasts cultured for 21 days using the RNeasy Micro Kit (Qiagen) according to the manufacturer's instructions. 0.5 mg of total RNA were used in a one-step RT-PCR system (Superscript III One-step RT-PCR system with platinum Taq, Invitrogen). The primer sequences for osteocalcin were as follows: 5′-GAAGCCCAGCGGTGCA-3′ and 5′-TGGGAGCAGCTGGGATGATG-3′. The PCR products were analyzed on a 1.5% agarose gel. The primer pair amplified a DNA band of 370 bp.

3. Results and discussions

3.1. Characterization of shRNA-functionalized calcium phosphate nanoparticles

First, shRNA-functionalized calcium phosphate nanoparticles were prepared by rapid mixing of aqueous solutions of calcium and phosphate salts and immediate functionalization of the nanocrystals with shRNA to prevent the aggregation of nanoparticles [17]. These nanoparticles carried a negative charge due to the negatively charged nucleic acids on their surface. The nucleic acids provided both electrostatic and steric stabilization of the particles and prevented their aggregation. The additional shells of calcium phosphate and shRNA provide not only stabilization of the particles, but also an additional protection for the shRNA incorporated into the first shell against endocellular nucleases, thus providing much higher silencing activity [17].

Scanning electron microscopy (SEM) showed spherical particles with a particle size of 100–250 nm for both kinds of shRNA nanoparticles (Fig. 1). This was confirmed by dynamic light scanning (DLS) which also showed that the particles were not agglomerated. The zeta potential of the nanoparticles was clearly negative (about −25 mV).

3.2. QCM analysis

The polyelectrolyte multilayer system was based on nanoparticles and sequentially deposited PLL. The assembly of (PLL–NP)$_n$-multilayered films was monitored by means of a dissipation-enhanced quartz crystal microbalance (QCM) (Fig. 2). The evolution of $\Delta f/\nu$ showed a regular film deposition starting with the first layer of PLL. The increase in $-\Delta f/\nu$ with the number of deposited layers suggested that regular film deposition occurred.

3.3. AFM analysis

In the next step, atomic force microscopy (AFM) was used to get additional information about the structure of these LbL architectures. In Fig. 3, a film made of alternating layers of PLL and nanoparticle was examined in situ by AFM in the liquid phase. The film thickness was evaluated by scratching the film with the AFM tip and estimated to 20 nm for the deposited materials.

3.4. Gene silencing

To test gene inhibition abilities of the nanoparticles embedded into the polyelectrolyte multilayer system, HOb cells were seeded on the (PLL–NP)$_1$ and on the (PLL–NP)$_6$ multilayer films. To determine the gene silencing efficiency of our system we analyzed the expression of osteocalcin by RT-PCR after the cells were brought in contact with shRNA nanoparticles, either in dispersion or incorporated into the multilayered film (Fig. 4). Our results clearly indicate that when incorporated into the multilayered film, the shRNA nanoparticles induced a much stronger inhibition of the osteocalcin expression than the dispersed nanoparticles.

For further characterization, the expression of osteopontin and osteocalcin in HOb cells was detected by immunofluorescence and the nuclei were visualized by Hoechst 33258 staining (Fig. 5). Osteopontin and osteocalcin were not inhibited in the untreated cells (Fig. 5A and B). In the case of the free shRNA (osteopontin) and shRNA (osteocalcin) in solution, the gene expression was also not inhibited (Fig. 5C and D). In the case of the dispersed nanoparticles, some inhibition of osteopontin and osteocalcin was observed (Fig. 5E and F). When the nanoparticles were incorporated into the multilayered film (PLL–NP)$_1$, the expression of osteopontin and osteocalcin was clearly inhibited (Fig. 5G and H), but in the case of (PLL–NP)$_6$, the expression of osteopontin and osteocalcin was fully inhibited (Fig. 5I and J).

4. Conclusions

The major challenge for this approach was to find an efficient method for shRNA delivery into cells. Using the multilayered films, we can incorporate more than one active molecule (DNA or siRNA for example) at the different levels, which act as a reservoir for cells and can be released slowly. In this case we reach a gradual and prolonged therapeutic effect. We can also get a more specific and sequential response by incorporation of smaller amounts of active molecules at different depth than the one obtained after treatment of cells in solution. We report here the first demonstration of a multilayered films-based delivery system containing nanoparticles for gene silencing of osteopontin and osteocalcin which are specific for bone cells. A new strategy based on a multi-shell calcium phosphate multilayered films for gene silencing of bone extracellular matrices was brought forward. This new strategy can be used to efficiently control the bone formation and could be applicable in tissue engineering.

Appendix

Figures with essential color discrimination. Most of the figures in this article have parts that are difficult to interpret in black and white. The full color images can be found in the on-line version, at doi:10.1016/j.biomaterials.2010.04.024.

References

[1] Schreier H. The new frontier: gene and oligonucleotide therapy. Pharm Acta Helv 1994;68(3):145–59.
[2] Leung RK, Whittaker PA. RNA interference: from gene silencing to gene-specific therapeutics. Pharmacol Ther 2005;107(2):222–39.
[3] Fire AZ. Gene silencing by double-stranded RNA. Angew Chem Int Ed 2007;46(37):6966–84.

[4] Kurreck J. RNA interference: from basic research to therapeutic applications. Angew Chem Int Ed 2009;48(8):1378–98.

[5] Manjunath N, Wu H, Subramanya S, Shankar P. Lentiviral delivery of short hairpin RNAs. Adv Drug Deliv Rev 2009;61(9):732–45.

[6] Tripathy SK, Black HB, Goldwasser E, Leiden JM. Immune responses to transgene-encoded proteins limit the stability of gene expression after injection of replication-defective adenovirus. Nat Med 1996;2(5):545–50.

[7] Van den Haute C, Eggermont K, Nuttin B, Debyser Z, Baekelandt V. Lentiviral vector-mediated delivery of short hairpin RNA results in persistent knockdown of gene expression in mouse brain. Hum Gene Ther 2003;14 (18):1799–801.

[8] Chirila TV, Rakoczy PE, Garrett KL, Lou X, Constable IJ. The use of synthetic polymers for delivery of therapeutic antisense oligodeoxynucleotides. Biomaterials 2002;23(2):321–42.

[9] Gill JS, Zhu X, Moore MJ, Lu L, Yaszemski MJ, Windebank AJ. Effects of NFkappaB decoy oligonucleotides released from biodegradable polymer microparticles on a glioblastoma cell line. Biomaterials 2002;23(13):2773–81.

[10] Zohra FT, Chowdhury EH, Akaike T. High performance mRNA transfection through carbonate apatite-cationic liposome conjugates. Biomaterials 2009;30(23–24):4006–13.

[11] McNeil SE, Perrie Y. Expert Opin Ther Pat 2006;16:1371–82.

[12] Rea JC, Gibly RF, Barron AE, Shea LD. Self-assembling peptide-lipoplexes for substrate-mediated gene delivery. Acta Biomater 2009;5(3):903–12.

[13] Moore NM, Sheppard CL, Sakiyama-Elbert SE. Characterization of a multifunctional PEG-based gene delivery system containing nuclear localization signals and endosomal escape peptides. Acta Biomater 2009;5(3):854–64.

[14] Sokolova V, Epple M. Inorganic nanoparticles as carriers of nucleic acids into cells. Angew Chem Int Ed 2008;47(8):1382–95.

[15] Kovtun A, Heumann R, Epple M. Calcium phosphate nanoparticles for the transfection of cells. Biomed Mater Eng 2009;19(2–3):241–7.

[16] Sokolova VV, Radtke I, Heumann R, Epple M. Effective transfection of cells with multi-shell calcium phosphate-DNA nanoparticles. Biomaterials 2006;27 (16):3147–53.

[17] Sokolova V, Kovtun A, Prymak O, Meyer-Zaika W, Kubareva EA, Romanova EA, et al. Functionalisation of calcium phosphate nanoparticles by oligonucleotides and their application for gene silencing. J Mater Chem 2007;17 (8):721–7.

[18] Epple M, Ganesan K, Heumann R, Klesing J, Kovtun A, Neumann S, et al. Application of calcium phosphate nanoparticles in biomedicine. J Mater Chem 2010;20:18–23.

[19] Dorozhkin SV, Epple M. Biological and medical significance of calcium phosphates. Angew Chem Int Ed 2002;41(17):3130–46.

[20] Decher G. Fuzzy nanoassemblies: toward layered polymeric multicomposites. Science 1997;277:1232–7.

[21] Berth G, Voigt A, Dautzenberg H, Donath E, Mohwald H. Polyelectrolyte complexes and layer-by-layer capsules from chitosan/chitosan sulfate. Biomacromolecules 2002;3(3):579–90.

[22] Hiller J, Mendelsohn JD, Rubner MF. Reversibly erasable nanoporous antireflection coatings from polyelectrolyte multilayers. Nat Mater 2002;1 (1):59–63.

[23] Jessel NB, Schwinte P, Donohue R, Lavalle P, Boulmedais F, Darcy R, et al. Pyridylamino-beta-cyclodextrin as a molecular chaperone for lipopolysaccharide embedded in a multilayered polyelectrolyte architecture. Adv Funct Mater 2004;14(10):963–9.

[24] Lvov Y, Onda M, Ariga K, Kunitake T. Ultrathin films of charged polysaccharides assembled alternately with linear polyions. J Biomater Sci Polym Ed 1998;9(4):345–55.

[25] Sato K, Suzuki I, Anzai J. Preparation of polyelectrolyte-layered assemblies containing cyclodextrin and their binding properties. Langmuir 2003;19 (18):7406–12.

[26] Serizawa T, Yamaguchi M, Akashi M. Enzymatic hydrolysis of a layer-by-layer assembly prepared from chitosan and dextran sulfate. Macromolecules 2002;35(23):8656–8.

[27] Kempf M, Mandal B, Jilek S, Thiele L, Voros J, Textor M, et al. Improved stimulation of human dendritic cells by receptor engagement with surface-modified microparticles. J Drug Target 2003;11(1):11–8.

[28] Jessel N, Atalar F, Lavalle P, Mutterer J, Decher G, Schaaf P, et al. Bioactive coatings based on a polyelectrolyte multilayer architecture functionalized by embedded proteins. Adv Mater 2003;15(9):692–5.

[29] Mendelsohn JD, Yang SY, Hiller J, Hochbaum AI, Rubner MF. Rational design of cytophilic and cytophobic polyelectrolyte multilayer thin films. Biomacromolecules 2003;4(1):96–106.

[30] Jewell CM, Zhang J, Fredin NJ, Lynn DM. Multilayered polyelectrolyte films promote the direct and localized delivery of DNA to cells. J Control Release 2005;106(1–2):214–23.

[31] Meyer F, Ball V, Schaaf P, Voegel JC, Ogier J. Polyplex-embedding in polyelectrolyte multilayers for gene delivery. Biochim Biophys Acta 2006;1758(3):419–22.

[32] Zhang X, Sharma KK, Boeglin M, Ogier J, Mainard D, Voegel JC, et al. Transfection ability and intracellular DNA pathway of nanostructured gene-delivery systems. Nano Lett 2008;8(8):2432–6.

[33] Jessel N, Oulad-Abdeighani M, Meyer F, Lavalle P, Haikel Y, Schaaf P, et al. Multiple and time-scheduled in situ DNA delivery mediated by beta-cyclodextrin embedded in a polyelectrolyte multilayer. Proc Natl Acad Sci U S A 2006;103(23):8618–21.